Nickel L-Edge Soft X-ray Spectroscopy of Nickel−Iron Hydrogenases and Model Compounds—Evidence for High-Spin Nickel(II) in the Active Enzyme

Hongxin Wang,[†] C. Y. Ralston,[†,‡] D. S. Patil,[§] R. M. Jones,[§] W. Gu,[†] M. Verhagen,[||] M. Adams,[||] P. Ge,[⊥] C. Riordan,[⊥] C. A. Marganian,[▽] P. Mascharak,[▽] J. Kovacs,[○] C. G. Miller,[#] T. J. Collins,[#] S. Brooker,[△] P. D. Croucher,[△] Kun Wang,[◇] E. I. Stiefel,[◇] and S. P. Cramer*[,†,§]

Contribution from the Department of Applied Science, University of California, Davis, California 95616, Lawrence Berkeley National Laboratory, Berkeley, California 94720, Department of Biochemistry, University of Georgia, Athens, Georgia 55455, Department of Chemistry, University of Delaware, Newark, Delaware 19716, Department of Chemistry, University of California, Santa Cruz, California 95064, Department of Chemistry, University of Washington, Seattle, Washington 98195, Department of Chemistry, Carnegie Mellon University, Pittsburgh, Pennsylvania 15213, Department of Chemistry, University of Otago, Dunedin, New Zealand, and Exxon Research and Engineering Company, Annandale, New Jersey 08801

Received March 16, 2000

Abstract: L-edge X-ray absorption spectroscopy has been used to study, under a variety of conditions, the electronic structure of Ni in the Ni−Fe hydrogenases from *Desulfovibrio gigas*, *Desulfovibrio baculatus*, and *Pyrococcus furiosus*. The status of the enzyme films used for these measurements was monitored by FT-IR spectroscopy. The L-edge spectra were interpreted by ligand field multiplet simulations and by comparison with data for Ni model complexes. The spectrum for Ni in *D. gigas* enzyme "form A" is consistent with a covalent Ni(III) species. In contrast, all of the reduced enzyme samples exhibited high spin Ni(II) spectra. The significance of the Ni(II) spin state for the structure of the hydrogenase active site is discussed.

Introduction

Ni−Fe hydrogenases catalyze both the oxidation and formation of molecular hydrogen.[1−5] They contain a single Ni−Fe active site, as well as one or more Fe−S clusters involved in electron transfer. Ni−Fe hydrogenases are generally heterodimeric proteins consisting of small (S) and large (L) subunits. Spectroscopy and crystallographic data on the *D. gigas* enzyme have shown that the small subunit contains one $[Fe_3S_4]^{1+/0}$ and two $[Fe_4S_4]^{2+/1+}$ clusters, while the large subunit contains the Ni−Fe center.[6]

In the crystal structure of the oxidized, "unready" *D. gigas* enzyme, the Ni is ligated by sulfurs from four cysteine residues and an additional ligand tentatively assigned as a μ-oxo species (Scheme 1).[7,11] The oxygen and two of the sulfur ligands bridge the Ni to a unique low-spin Fe center at 2.9 Å.[7] This Fe is also ligated by three nonprotein diatomic ligands, identified by infrared studies as one CO and two CN.[4,12] In contrast, in the oxidized *D. vulgaris* Miyazaki structure the nonprotein bridging ligand is assigned as a sulfur species, the Ni−Fe distance is 2.55 Å, and one of the diatomic Fe ligands is an SO molecule.[9] Garcin and co-workers have suggested that the shorter Ni−Fe distance might be due to a larger fraction of "ready" form in the latter crystals.[8]

There is less disagreement over the structure of the reduced, active form of the enzyme. In the structure of the *D. baculatum* enzyme, the tightly bound bridging ligand has disappeared, and the Ni−Fe distance has contracted to 2.5 Å.[8] In the reduced *D. vulgaris* structure, although one of the diatomics is still assigned as SO, the monatomic sulfur bridge has also disappeared and the Ni−Fe distance is 2.59 Å.[10]

* To whom the correspondence should be addressed.
[†] University of California, Davis.
[‡] Current address: Department of Biophysics and Physiology, Albert Einstein College of Medicine, Yeshiva University, The Bronx, NY 10461.
[§] Laurence Berkeley National Laboratory.
[||] University of Georgia.
[⊥] University of Delaware.
[▽] University of California, Santa Cruz.
[○] University of Washington.
[#] Carnegie Mellon University.
[△] University of Otago.
[◇] Exxon Research and Engineering Co.

(1) Fontecilla-Camps, J. C. *Struct. Bonding* **1998**, *91*, 2−30.
(2) Fontecilla-Camps, J. C.; Frey, M.; Garcin, E.; Hatchikian, C.; Montet, Y.; Piras, C.; Vernede, X.; Volbeda, A. *Biochemie* **1997**, *79*, 661−666.
(3) Frey, M. *Struct. Bonding* **1998**, *90*, 97−126.
(4) Happe, R. P.; Roseboom, W.; Pierik, A. J.; Albracht, S. P. J.; Bagley, K. A. *Nature* **1997**, *385*, 126.
(5) Montet, Y.; Garcin, E.; Volbeda, A.; Hatchikian, C.; Frey, M.; Fontecilla-Camps, J. C. *Pure Appl. Chem.* **1998**, *70*, 25−31.
(6) Moura, J. J. G.; Teixeira, M.; Moura, I.; LeGall, J. In *The Bioinorganic Chemistry of Nickel*; Lancaster, J. R., Ed.; VCH Publishers: New York, 1988; Chapter 9, p 191.
(7) Volbeda, A.; Garcin, E.; Piras, C.; de Lacey, A. L.; Fernandez, V. M.; Hatchikian, E. C.; Frey, M.; Fontecilla-Camps, J. C. *J. Am. Chem. Soc.* **1996**, *118*, 12989−12996.
(8) Garcin, E.; Vernede, X.; Hatchikian, E. C.; Volbeda, A.; Frey, M.; Fonecilla-Camps, J. C. *Struct. Folding Des.* **1999**, *5*, 557−566.
(9) Higuchi, Y.; Yagi, T.; Yasuoka, N. *Structure* **1997**, *5*, 1671−1680.
(10) Higuchi, Y.; Ogata, H.; Miki, K.; Yasuoka, N.; Yagi, T. *Struct. Folding Des.* **1999**, *7*, 549−556.
(11) Volbeda, A.; Charon, M. H.; Piras, C.; Hatchikian, E. C.; Frey, M.; Fontecilla-Camps, J. C. *Nature* **1995**, *373*, 580−587.
(12) Bagley, K. A.; Duin, E. C.; Roseboom, W.; Albracht, S. P. J.; Woodruff, W. H. *Biochemistry* **1995**, *34*, 5527−5535.

10.1021/ja000945g CCC: $19.00
Published on Web 10/11/2000

Scheme 1. Generalization of Structures Proposed for the Ni−Fe Site in Oxidized and Reduced Hydrogenases[7−10] (Left) and Relationships between Different Forms of Hydrogenase throughout the Catalytic Cycle (Right)[a]

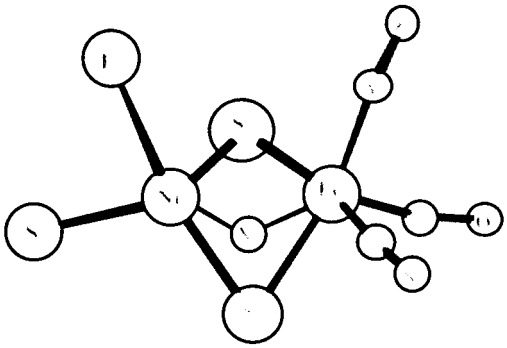

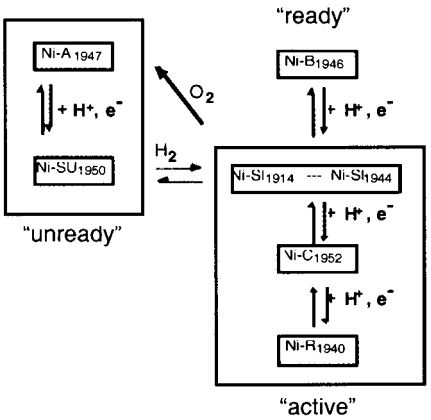

[a] S and E represent cysteine S ligands, except in *D. baculatum*, where E is a selenocysteine Se ligand. X is only observable in the oxidized structures; it is assigned as μ-O or μ-OH in the *D. gigas* structure and as S in *D. vulgaris*. Y−Z is a CN^- ligand in *D. gigas*; it is proposed to be SO in *D. vulgaris*.

The hydrogenase Ni−Fe center exhibits a range of EPR-active and EPR-silent states, and the electronic structures of these forms have also been controversial.[6,13−15] The *D. gigas* enzyme is isolated aerobically as a mixture containing two catalytically inactive species—the Ni-A, or "unready" form, and the Ni-B, or "ready" form. Both Ni-A and Ni-B exhibit $S = {}^1/_2$ EPR signals and are most often described as Ni(III) complexes, but Ni(II)−thiyl radical assignments have also been proposed.[16] Activation of the Ni-A and Ni-B forms with hydrogen puts the Ni in a manifold of three active species. The highest potential catalytic form is referred to as the "silent intermediate" or Ni-SI. At a lower potential is another EPR detectable state, termed Ni-C.[17] Complete reduction yields another EPR silent state termed Ni-R.

De Lacey and co-workers have shown that Ni-B, Ni-SI, Ni-C, and Ni-R can be smoothly interconverted in redox titrations and that each species has characteristic CO and CN stretching frequencies.[18] Lindahl and co-workers have attempted to quantify the number of electrons involved in each step of the catalytic cycle. Their results suggest that the Ni-R state is one electron more reduced than Ni-C, that Ni-C is more reduced than Ni-B, and that Ni-C and Ni-B states are separated by at least one EPR silent state.[19−21]

The oxidation state of Ni in the Ni-B, Ni-SI, Ni-C, and Ni-R sequence has been the subject of numerous proposals, including respectively Ni(III)−Ni(II)−Ni(I)−Ni(0),[22] Ni(III)−Ni(II)−Ni(I)−Ni(I),[13,14] and Ni(III)−Ni(II)−Ni(III)−Ni(II).[6,23] It has also been proposed that the redox chemistry is centered on the ligands.[16] Recent density functional calculations describe a Ni−Fe(II,III) resting state, presumably related to form SI, which can be reduced by two electrons to a Ni−Fe(I,II) oxidation level.[24]

Previous K-edge XANES studies of Ni−Fe hydrogenases have shown only small changes between different enzyme forms. Shifts in the *D. gigas* hydrogenase K-edge were interpreted to indicate that Ni is reduced from Ni(III) in the native state to Ni(II) upon reduction by hydrogen.[25] K-edge studies on *Thiocapsa roseopersicina* hydrogenase in forms A, B, C, SI, and R showed no significant shifts in nickel edge position, suggesting a ligand-based redox chemistry.[16] A comparison of forms C and L also found no significant spectral difference.[26] More recent Ni K-edge XAS studies of the oxidized and reduced forms of several hydrogenases were interpreted to indicate at most a one-electron reduction of the Ni centers, but no specific oxidation states were proposed.[27]

L-edge X-ray measurements can provide information that is complementary to K-edge XANES and EPR spectroscopy.[28,29] We have previously used this technique to study the electronic structure of Ni in rubredoxin,[30] in the hydrogenase from *Pyrococcus furiosus*,[31] and in carbon monoxide dehydrogenase.[32] In this paper, L-edge spectra for the Ni−Fe hydrogenases

(13) Cammack, R.; Rao, K. K.; Serra, J.; Llama, M. J. *Biochimie* **1986**, *68*, 93.
(14) Cammack, R. *Adv. Inorg. Chem.* **1988**, *32*, 297.
(15) Teixeira, M.; Moura, I.; Xavier, A. V.; Huynh, B. H.; Dervartanian, D. V.; Peck, H. D.; LeGall, J.; Moura, J. J. G. *J. Biol. Chem.* **1985**, *260*, 8942−8950.
(16) Bagyinka, C.; Whitehead, J. P.; Maroney, M. J. *J. Am. Chem. Soc.* **1993**, *115*, 3576−3585.
(17) LeGall, J.; Ljungdahl, P. O.; Moura, I.; Peck, H. D.; Xavier, A.; Moura, J. J. G.; Teixeira, M.; Huynh, B. H.; DerVartanian, D. V. *Biochem. Biophys. Res. Commun.* **1982**, *106*, 610−615.
(18) de Lacey, A. L.; Hatchikian, E. C.; Volbeda, A.; Frey, M.; Fontecilla-Camps, J. C.; Fernandez, V. M. *J. Am. Chem. Soc.* **1997**, *119*, 7181−7189.
(19) Roberts, L. M.; Lindahl, P. A. *Biochemistry* **1994**, *33*, 14339−14350.
(20) Barondeau, D. P.; Roberts, L. M.; Lindahl, P. A. *J. Am. Chem. Soc.* **1994**, *116*, 3442−3448.
(21) Roberts, L. M.; Lindahl, P. A. *J. Am. Chem. Soc.* **1995**, *117*, 2565−2572.
(22) van der Zwaan, J. W.; Albracht, S. P. J.; Fontijn, R. D.; Slater, E. C. *FEBS Lett.* **1985**, *179*, 271.
(23) Moura, J. J. G.; Teixeira, M.; Moura, I. *Pure. Appl. Chem.* **1989**, *61*, 915.
(24) Pavlov, M.; Siegbahn, P. E. M.; Blomberg, M. R. A.; Crabtree, R. H. *J. Am. Chem. Soc.* **1998**, *120*, 548−555.
(25) Scott, R. A.; Wallin, S. A.; Czechowski, M.; Dervartanian, D. V.; LeGall, J.; Peck, H. D. J.; Moura, I. *J. Am. Chem. Soc.* **1984**, *106*, 6864−6865.
(26) Whitehead, J. P.; Gurbiel, R. J.; Bagyinka, C.; Hoffman, B. M.; Maroney, M. J. *J. Am. Chem. Soc.* **1993**, *115*, 5629−5635.
(27) Gu, Z. J.; Dong, J.; Allan, C. B.; Choudhury, S. B.; Franco, R.; Moura, J. J. G.; Legall, J.; Przybyla, A. E.; Roseboom, W.; Albracht, S. P. J.; Axley, M. J.; Scott, R. A.; Maroney, M. J. *J. Am. Chem. Soc.* **1996**, *118*, 11155−11165.
(28) deGroot, F. M. F.; Fuggle, J. C.; Thole, B. T.; Sawatzky, G. A. *Phys. Rev. B* **1990**, *42*, 5459−5468.
(29) Cramer, S. P.; Wang, H.; Bryant, C.; Legros, M.; Horne, C.; Patel, D.; Ralston, C.; Wang, X. In *Spectroscopic Methods in Bioinorganic Chemistry*; Solomon, E. I., Hodgson, K. O., Eds.; American Chemical Society: Washington, DC, 1998.
(30) van Elp, J.; Peng, G.; Searle, B. G.; Mitra-Kirtley, S.; Huang, Y. H.; Johnson, M. K.; Zhou, Z. H.; Adams, M. W. W.; Maroney, M. J.; Cramer, S. P. *J. Am. Chem. Soc.* **1994**, *116*, 1918−1923.
(31) van Elp, J.; Peng, G.; Zhou, Z. H.; Adams, M. W. W.; Baidya, N.; Mascharak, P. K.; Cramer, S. P. *Inorg. Chem.* **1995**, *34*, 2501−2504.
(32) Cramer, S. P.; Ralston, C. Y.; Wang, H. X.; Bryant, C. *J. Electron Spectrosc. Relat. Phenom.* **1997**, *86*, 175−183.

from *D. gigas*, *D. baculatus*, and *Pyrococcus furiosus* are reported, along with FT-IR spectra used to monitor the redox status of the samples. The L-edge data are interpreted both by comparison with model compound spectra and with theoretical simulations. Complementary results on CO dehydrogenase are reported in a companion paper.[33]

Experimental Section

Hydrogenase Isolation. The *Desulfovibrio* enzymes were purified by ion-exchange chromatography from bacteria grown on a sulfate−lactate medium.[34,35] The samples were treated anaerobically with reductants and inhibitors using a vacuum manifold.[35] A hydrogen evolution assay was performed by the method of Peck and Gest[36] using a gas chromatograph equipped with a molecular sieve column. The specific activity was estimated by measuring the hydrogen gas evolved in a reaction with methylviologen as electron carrier and dithionite as reductant (pH 8.0). The *P. furiosus* enzyme samples were prepared by anaerobic chromatographic techniques.[37]

Preparation of Model Compounds. The Ni model compounds used for this investigation and the companion paper[33] were synthesized according to published procedures as referenced: $[Ni(tren)_2](BF_4)_2$,[38] Ni^{I}diene(ClO_4), and Ni^{II}diene$(ClO_4)_2$, diene = 5,7,7,12,14,14-hexamethyl-1,4,8,11-tetraazacyclotetradeca-4,11-diene);[39] Na[Ni^{I}"S_4"] and Ni^{II}"S_4", "S_4" represents bis(diphenylbis((methylthio)methyl)borate),[40] $Ni^{II}L_{s5}$ (L_{s5} = (−S-*o*-$C_6H_4SC_2H_4)_2$S);[41] Ni^{I}TMC(ClO_4) (TMC = 1,4,8,-11-tetramethyl-1,4,8,11-tetraazacyclotetradecane);[42] $Ni^{II}L_{S2}$(Me)N_3(Pr),[43] $(Ph_4P)_2Ni^{II}$mac*,[44] and $(Ph_4P)[Ni^{III}DCB]$,[44] $(Et_4N)_2[Ni^{II}$pdtc] and $(Et_4N)[Ni^{III}pdtc_2]$ (pdtc = pyridine-2,6-bis(thiocarboxylate)) [Kruger, 1987, #255]; Ni^{II}(DAPA)Cl_2, Ni^{II}(terpy)(2,4,6-$(Me)_3C_6H_2Se)_2$, and Ni^{II}(DAPA)$(SePh)_2$,[45] Ni^{III}(cyclam)$Cl_2(ClO_4)$,[46] Ni^{II}(cyclam)$(ClO_4)_2$,[47] Li[Ni^{III}(κ^4-mac*)], where (κ^4-mac*) is peralkylated (*) *m*acrocyclic poly*a*nionic *c*helating ligand = 13,13-diethyl-2,2,5,5,7,7,10,10-octamethyl-3,6,9,12,14-pentaoxo-1,4,8,11-tetraazacyclotetradecane,[48] K_3NiF_6,[49] [Ni^{II}_2"LS1"] $(ClO_4)_2$, where "LS1" represents a ligand derived from condensation of 2,6-diformyl-4-methylthiophenolate and 1,3-diaminopropane,[50] (*n*-Bu_4N)[$Ni(S_2C_2(CF_3)_2)_2$],[51] and $(Et_4N)[Ni(S_2C_2$-$Ph_2)_2]$.[52] NiO and NiF_2 were purchased from Aldrich Chemical Co. The Ni/MgO sample was obtained from Goodfellow Metals; it consisted of 1400 ppm by weight Ni doped into a MgO crystal.

Model compounds (except the Ni/MgO crystal) were ground to a fine powder in a Vacuum Atmospheres glovebox under a N_2 atmosphere and attached to sample holders using double-sided adhesive tape. Additional details about the model spectra are provided as Supplementary Model in the companion paper.[33]

Preparation and Assay of Hydrogenase Films. Hydrogenase films for L-edge experiments were prepared by syringing a drop (∼20 μL) of a protein solution onto a silicon or sapphire substrate and allowing it to dry under the appropriate atmosphere in an anaerobic chamber. All solutions were initially buffered at pH 7.8 with 0.1 M Tris-HCl. The film samples were transferred anaerobically to the vacuum chamber via a load-lock.

D. gigas hydrogenase films were made from solutions ∼15 mg/mL in protein. In typical assays, before film preparation the *D. gigas* enzyme in the as-isolated state had a specific activity of 500 ± 50 μM H_2·min^{-1}·mg^{-1}. After drying on a silicon substrate (and redissolving the same material), the measured activity was 450 ± 50 μM H_2·min^{-1}·mg^{-1}, and after the X-ray measurements, the activity was 400 ± 50 μM H_2·min^{-1}·mg^{-1}. Hydrogen-reduced *D. gigas* films were prepared by incubation of the enzyme solution under pure H_2 for 8 h and drying under a H_2 or N_2 atmosphere. Essentially the same activities were recorded for the hydrogen-reduced samples as for the as-isolated material.

D. baculatus films were made from enzyme solutions approximately ∼15 mg/mL in protein. The initial activity of the *D. baculatus* hydrogenase in the as-isolated state was 700 ± 100 μM H_2·min^{-1}·mg^{-1}. After drying on a silicon substrate the activity was 650 ± 100 μM H_2·min^{-1}·mg^{-1}, and the same activity was measured after the L-edge measurements. Hydrogen-reduced *D. baculatus* samples were prepared by incubation under H_2 for 8 h. Measured activities of the reduced samples were 650 ± 50, 600 ± 50, and 500 ± 50 μM H_2·min^{-1}·mg^{-1} for the solution, film, and film exposed to X-rays, respectively.

During the course of this work, questions were raised about possible sample changes when the "bare" protein films are exposed to vacuum. To address these concerns, additional protein spectra were recorded on "sealed" or "capped" samples. In the case of the sealed samples, the samples were covered with a 5000-Å silicon nitride membrane before introduction to the vacuum chamber and throughout the X-ray measurement. The capped samples were prepared as films and then sealed in a vacuum-tight enclosure under H_2, N_2, or CO as appropriate. These samples were only exposed to vacuum after transfer through the load-lock and equilibration with the 20 K coldfinger. Additional details are reported in the companion paper.[33]

FT-IR Spectroscopy of Hydrogenase Films. During the latter phase of this project, we were able to record FT-IR and X-ray spectra on the same samples, by preparing the films on a sapphire substrate. For bare and capped samples, the FT-IR data were collected on the same samples (on sapphire) before and after the L-edge measurement. To keep these samples anaerobic during FT-IR analysis, a second sapphire window was placed on top of the film while inside an anaerobic box, and the two sapphire plates were sealed with an O-ring. For samples sealed behind the silicon nitride membrane, it was impossible to measure the sample FT-IR directly. Instead, the spectra were recorded on parallel samples from the same reaction batch. All FT-IR spectra were recorded at room temperature with 1-cm^{-1} resolution using a Mattson Infinity Series spectrophotometer with an InGaAs detector.

The sample films were approximately circular with an average diameter of 4−5 mm. For comparison, the soft X-ray beam was about 3 mm wide and 1 mm high, and the IR beam is approximately a 5 mm diameter circle. Although the samples were moved during data collection, so that the X-rays illuminated three or four different spots, there is no guarantee that the FT-IR and X-ray beams sampled the same area. Furthermore, the X-rays probe depth is ∼1 μm, while the FT-IR beam probes the entire depth of the sample. Although the FT-IR data do not rule out the possibility of radiation damage, they do prove that >90% of the sample remained in the same form before and after analysis in the vacuum chamber.

X-ray Data Collection. The samples were transferred anaerobically using a magnetic arm and loadlock to the spectroscopy vacuum

(33) Ralston, C. Y.; Wang, H.; Ragsdale, S. W.; Kumar, M.; Spangler, N. J.; Ludden, P. W.; Gu, W.; Jones, R. M.; Cramer, S. P. *J. Am. Chem. Soc.*, **2000**, *122*, 10553−10560.
(34) He, S. H.; Teixeira, M.; LeGall, J.; Patil, D. S.; Moura, I.; Moura, J. J. G.; DerVartanian, D. V.; Huynh, B. H.; Peck, H. D., Jr. *J. Biol. Chem.* **1989**, *264*, 2678−2682.
(35) Patil, D. S. *Methods Enzymol.* **1994**, *243*, 68−94.
(36) Peck Jr., H. D.; Gest, H. *J. Bacteriol.* **1965**, *71*, 70−73.
(37) Bryant, F. O.; Adams, M. W. W. *J. Biol. Chem.* **1989**, *264*, 5070.
(38) Colpas, G. J.; Kumer, M.; Day, R. O.; Maroney, M. J. *Inorg. Chem.* **1990**, *29*, 4779−4788.
(39) Lovecchio, F. V.; Gore, E. S.; Busch, D. H. *J. Am. Chem. Soc.* **1974**, *96*, 3109−3118.
(40) Ge, P. H.; Riordan, C. G.; Yap, G. P. A.; Rheingold, A. L. *Inorg. Chem.* **1996**, *35*, 5408−5409.
(41) Cha, M. Y.; Catlin, C. L.; Critchlow, S. C.; Kovacs, J. A. *Inorg. Chem.* **1993**, *32*, 5868−5877.
(42) Ram, M. S.; Riordan, C. G.; Ostrander, R.; Rheingold, A. L. *Inorg. Chem.* **1995**, *34*, 5884−5892.
(43) Shoner, S. C.; Olmstead, M. M.; Kovacs, J. A. *Inorg. Chem.* **1994**, *33*, 7−8.
(44) Collins, T. J.; Kostka, K. L.; Uffelman, E. S.; Weinberger, T. L. *Inorg. Chem.* **1991**, *30*, 4204−4210.
(45) Marganian, C. A.; Vazir, H.; Baidya, N.; Olmstead, M. M.; Mascharak, P. K. *J. Am. Chem. Soc.* **1995**, *117*, 1584−1594.
(46) Ito, T.; Sugimoto, M.; Toriumi, K.; Ito, H. *Chem. Lett.* **1981**, 1477−1478.
(47) Barefield, E. K.; Wagner, F.; Flerlinger, A. W.; Dahl, A. R. *Inorg. Synth.* **1976**, *16*, 220−225.
(48) Collins, T. J.; Nichols, T. R.; Uffelman, E. S. *J. Am. Chem. Soc.* **1991**, *113*, 4708−4709.
(49) Zemva, B.; Chacon, L.; Lutar, K.; Shen, C.; Allman, J.; Bartlett, N. *J. Fluorine Chem.* **1995**, *71*, 195−196.
(50) Brooker, S.; Croucher, P. D.; Roxburgh, F. M. *J. Chem. Soc., Dalton* **1996**, 3031−3037.
(51) Davison, A.; Holm, R. H. *Inorg. Synth.* **1967**, *10*, 8.
(52) Davison, A.; Edelstein, N.; Holm, R. H.; Maki, A. H. **1963**, *2*, 1227.

chamber, maintained at less than 5×10^{-9} Torr. They were mounted onto a gold-plated liquid helium cooled coldfinger, which was maintained at 20−30 K throughout the X-ray measurements. Model compound L-edge spectra were recorded using total electron yield detection[53] at beamline 8-2 at Stanford Synchrotron Radiation Laboratory[54] and at beamline 9.3.2 at the Advanced Light Source.[55] The photon energy resolution used for the measurements was on the order of 0.5 eV. The spectra were calibrated by using the total electron yield spectrum of either NiF_2 or NiO, using values for the absorption maxima of 852.7 and 853.2 eV, respectively.[56]

The protein spectra (and the Ni/MgO spectrum) were recorded at SSRL beamline 8−2 using fluorescence detection, either with a windowless 13-element germanium detector[57] or with a 30-element version of the same type of detector. The resolution was 1.2 ± 0.2 eV for capped and sealed samples and ∼0.5−1 eV for bare samples. The incident beam intensity was measured by recording the photocurrent from a gold-coated grid placed between the sample and the monochromator. Each protein spectrum represents the sum of approximately 40 20-min scans for bare and capped samples and 100 scans for sealed samples. Calibration samples were run hourly during protein scans to monitor beam stability and resolution. To minimize radiation damage, the position of the X-ray beam on the sample was moved every few scans. No evidence was observed for changes in the spectra over time.

Ligand Field Multiplet Calculations. Theoretical simulations of L-edge spectra were calculated for Ni^{1+}, Ni^{2+}, and Ni^{3+} using published methods.[28,56,58] Ligand field parameters 10 D_q, D_s, and D_t were adjusted to yield a good match between calculated and experimental spectra. The ab initio Hartree−Fock values of the Slater integrals and spin−orbit couplings (ξ_{2p} and ξ_{3d}) were used as tabulated.[59] Charge transfer effects were taken into account by a reduction of the Slater integrals in the calculation. The spectra were broadened by convolution with a Lorentzian and a Gaussian to describe the lifetime and instrumental broadening, respectively.[28]

Results

Overview of Model Compound Spectra. Soft X-ray L-edge spectroscopy is still a relatively novel technique for probing bioinorganic samples. For this reason, we illustrate some of the effects of oxidation state, spin state, and covalency in Figure 1. Ni L-edges generally shift to higher energy with higher oxidation state, by ∼1 eV/oxidation state. The average L_3 absorption centroids for Ni(I), Ni(II, HS/LS), and Ni(III) model compounds are at 852.5, 853.4/853.5, and 854.5 eV, respectively. Ni L-edges are split (by ∼17 eV) into L_3 ($2p_{1/2}$) and L_2 ($2p_{1/2}$) regions. Coulomb and exchange interactions between the core hole and the 3d shell are also significant—this gives rise to a "multiplet structure" that is often diagnostic of the 3d configuration. Of particular relevance for hydrogenase, (1) Ni(I) spectra do not exhibit multiplet structure (because the *d*-shell is full in the final state), (2) high-spin Ni(II) spectra generally have multiplet structure on the high energy side of the L_3 peak and broad or split L_2-edges, (3) low-spin Ni(II) spectra have little multiplet structure on the L_3 peak and relatively sharper and strong L_2-edges, and (4) ionic Ni(III) multiplet features occur on the low energy side of the L_3 peak, while covalent Ni(III) spectra have broad peaks without clear multiplet structure.

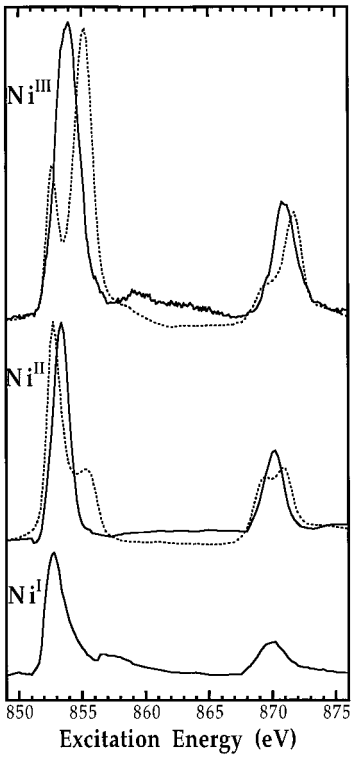

Figure 1. A survey of Ni model compound L-edge spectra. Top to bottom: (a) ionic vs covalent Ni(III): $Li[Ni^{III}(\kappa^4\text{-mac*})]$ (—) vs $[Ni^{III}(pdtc_2)]^-$ (- - -). (b) High-spin vs low-spin Ni(II): NiF_2 (—) vs Ni^{II}"S_4" (- - -). (c) $Na[Ni^I$"S_4"] (—).

FT-IR Spectra of Enzyme Films. To achieve the highest possible Ni concentration for the L-edge measurements, the spectra were recorded on partially dried hydrogenase films. FT-IR spectroscopy was used to monitor the redox status of these films. As illustrated in Figure 2, the IR bands observed for these films correlate well with solution spectro-electrochemical FT-IR studies of the *D. gigas* enzyme by de Lacey and co-workers.[18]

The FT-IR spectrum of the "as-isolated" *D. gigas* film (Figure 2) exhibits a dominant CO band at 1946 cm^{-1}, along with two clear CN stretches at 2082 and 2093 cm^{-1}. Essentially the same values were reported for the form A or "unready" state (1947, 2083, 2093 cm^{-1}).[7] By itself, the FT-IR cannot rule out the presence of some form B, which is reported to have bands at (1946, 2079, 2090 cm^{-1}).[7] However, in separate EPR experiments, we found no observable Ni-B in the EPR spectra. There is a shoulder at ∼1951 cm^{-1}, which most likely represents form SU or "unready-reduced" material. By fitting the FT-IR spectrum with two Gaussian components, and assuming equal absorption coefficients for both species, we estimate that the sample contains about 88% form A and ∼12% form SU. After the L-edge measurements, the FT-IR spectra of bare or capped samples showed ∼81% form A and ∼19% form SU. We cannot tell whether the apparent small amount of photoreduction occurred during the X-ray measurement or after sample removal from the cryostat and subsequent thawing.

The FT-IR spectra of a H_2-reduced sample confirms that films can be made which are a single species that resemble solution form R. (The best samples were reduced with H_2 and then dried under H_2 in the presence of a small amount of dithionite.) The main CO peak is at 1937 cm^{-1}, and there are CN peaks at 2060 and 2073 cm^{-1}. The CO peak is below the value of 1940 cm^{-1} reported for solution form R or "reduced" enzyme, but above

(53) Stöhr, J. *NEXAFS Spectroscopy* Springer-Verlag: New York, 1992.
(54) Terminello, L. J.; Waddill, G. D.; Tobin, J. G. *Nucl. Inst. Methods A* **1992**, *319*, 271−276.
(55) Hussain, Z.; Huff, W. R. A.; Keller, S. A.; Moler, E. J.; Heimann, P. A.; McKinney, W.; Padmore, H. A.; Fadley, C. S.; Shirley, D. A. *J. Electron Spectrosc. Relat. Phenom.* **1996**, *80*, 401−404.
(56) van der Laan, G.; Zaanen, J.; Sawatzky, G. A.; Karnatak, R.; Esteva, J.-M. *Phys. Rev. B* **1986**, *33*, 4253−4263.
(57) Cramer, S. P.; Chen, J.; George, S. J.; van Elp, J.; Moore, J.; Tench, O.; Colaresi, J.; Yocum, M.; Mullins, O. C.; Chen, C. T. *Nucl. Inst. Methods A* **1992**, *319*, 285−289.
(58) deGroot, F. M. F. *J. Electron Spectrosc. Relat. Phenom.* **1994**, *67*, 529−622.
(59) van der Laan, G.; Kirkman, I. W. *J. Phys.: Condens. Matter* **1992**, *4*, 4189−4204.

Figure 2. FT-IR spectra of hydrogenase films in different states and from different sources. Left: *D. gigas* enzyme in (a) as-isolated, before (—) and after (- - -) L-edge experiment, (b) H_2-reduced, before (—) and after (- - -) L-edge experiment, (c) dithionite-reduced, and (d) CO-inhibited states. Right: (e) as-isolated *D. baculatus*, (f) H_2-reduced *D. baculatus*, (g) as-isolated *P. furiosus*, and (h) H_2-reduced *P. furiosus* enzymes.

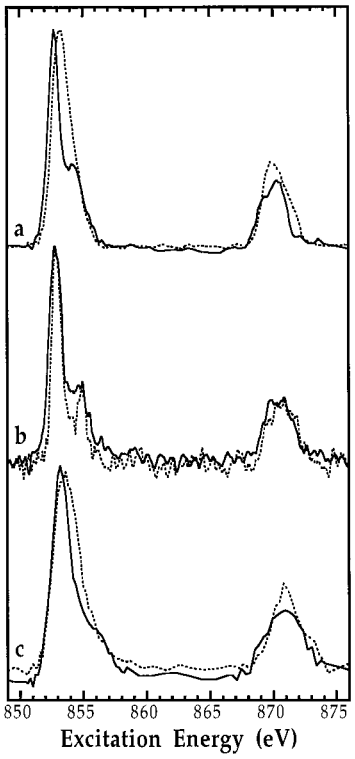

Figure 3. Survey of Ni−Fe H_2ase L-edge spectra on bare films. Top to bottom: (a) as-isolated *D. gigas* (- - -) compared with H_2-reduced *D. gigas* (—), (b) as-isolated *D. baculatus* (- - -) compared with H_2-reduced *D. baculatus* (—), and (c) 75 C thionine-oxidized *P. furiosus* (- - -) compared with H_2-reduced *P. furiosus* (—) enzymes.

the 1934 cm^{-1} peak assigned to form SI-2 or "silent intermediate".[18] (We note that the CO peak reported for the *C. vinosum* enzyme is at 1934 cm^{-1}.)[12] The CN peaks coincide exactly with the values reported for *D. gigas* form R,[18] and there is no evidence for a CN band at 2086 cm^{-1} that would indicate form SI-2. We conclude that H_2-reduced films are ∼95% in a single reduced species. To allow for a slight conformational difference with the solution form R, we label our sample "Ni−R_{film}". After the L-edge measurements, the FT-IR spectra indicated ∼88% Ni-R_{film} with ∼12% Ni-A,B.

The "dithionite-reduced" *D. gigas* film has an IR spectrum with a strong CO band at 1952 cm^{-1} and CN features at 2089 and 2099 cm^{-1} (Figure 2). Reduction (without H_2 activation) of the "unready" *D. gigas* protein has been shown to yield another "unready" species termed "silent, unready" or "SU" with a midpoint potential E_m' of −245 mV at pH 8.3.[18] It has essentially the same IR spectrum as our "dithionite-reduced" film sample, which therefore appears to be nearly homogeneous form SU.

In Figure 2 we also report the FT-IR spectrum of CO-inhibited *D. gigas* enzyme. The main CO peak is at 1932 cm^{-1}, with an additional CO peak at 2057 cm^{-1}. To our knowledge a solution spectrum for the CO-inhibited *D. gigas* enzyme has not been reported previously. The CO peaks correspond well with the 1929- and 2060-cm^{-1} values reported for *C. vinosum* hydrogenase.[60] Small amounts of forms R (29%) and SU (1%) appear to be present; by fitting the CO region we estimate the sample to be ∼70% CO-inhibited H_2ase.

FT-IR spectra for hydrogenases from *P. furiosus* and *D. baculatus* are also shown in Figure 2. To our knowledge, FT-IR spectra of these enzymes have not previously been reported. The as-isolated *Db* spectrum has a major peak at 1946 cm^{-1}, as well as a shoulder at 1951 cm^{-1} and a minor peak at 1937 cm^{-1}. Hydrogen reduction changes the relative intensities, so that the 1951-cm^{-1} peak is the dominant species. According to the literature, this enzyme does not exhibit a form A EPR signal, and it does not require hydrogen activation after purification.[61] It is tempting to assign the 1951-cm^{-1} peak as form C, since the CO peaks for *C. vinosum* and *D. gigas* occur at 1950 and 1952 cm^{-1}, respectively. A more detailed assignment of the spectra is in progress. Since the films are clearly heterogeneous, we can only make qualitative conclusions from the corresponding L-edge spectra.

The *P. furiosus* hydrogenase FT-IR spectra indicate a surprising amount of heterogeneity in these samples. There are at least five significant components in the CO stretch region—1966, 1959, 1952, 1941, and 1935 cm^{-1}. Upon hydrogen reduction of the as-isolated enzyme, there is a shift in the dominant peak from 1959 to 1941 cm^{-1}. The enzyme is isolated anaerobically under reducing conditions;[37] this shift to 1941 cm^{-1} might correspond to an increase in the concentration of a form R species. A more detailed analysis is beyond the scope of this paper. The spectra indicate that the composition of the films is far more complex than originally appreciated.[31]

Enzyme L-Edge Spectra Overview. The general similarity of L-edges for reduced hydrogenases from different species, as well as the clear differences observed between reduced and oxidized forms, are illustrated in Figure 3. The as-isolated *D. gigas* spectrum has a broad L_3 maximum near 853.5 eV and a

(60) Bagley, K. A.; Vangarderen, C. J.; Chen, M.; Duin, E. C.; Albracht, S. P. J.; Woodruff, W. H. *Biochemistry* **1994**, *33*, 9229−9236.

(61) Teixeira, M.; Moura, I.; Xavier, A. V.; Huynh, B. H.; Dervartanian, D. V.; Peck, H. D.; LeGall, J.; Moura, J. J. G. *Eur. J. Biochem.* **1987**, *26*, 47−58.

relatively sharp L_2 edge, while H_2-reduced *D. gigas* has a primary L_3 peak near 853.2 eV, along with a weaker and broader L_2 edge. The centroid shifts from 853.35 to 854.0 eV between reduced and as-isolated samples. For Ni(II) and Ni(III) complexes with the same ligand, typical shifts are ~1 eV for ionic complexes such as $[Ni^{II,III}(cyclam)]^{2+,3+}$ and 0.6 eV for covalent species such as $[Ni^{II,III}pdtc_2]^{2-,-}$.[30,31,33] The L_3 absorption maxima for Ni(II) compounds generally range between 853.2 and 853.9 eV. Thus, the changes observed between H_2-reduced and as-isolated *D. gigas* spectra are consistent with the oxidation of a Ni(II) complex to a very covalent Ni(III) species, but without additional evidence they could also be interpreted as a Ni(II) species changing from a covalent to a more ionic environment.

The L-edge spectra for H_2-reduced *D. baculatus* and *P. furiosus* proteins resemble the corresponding *D. gigas* spectrum. They all exhibit features on the high energy side of the main L_3 peak and broad or even split L_2-edges. This spectral pattern arises from multiplet interactions and is characteristic of high-spin Ni(II).[30,62] We now compare some of these spectra with model compounds and simulate the features in more detail.

Oxidized *D. gigas* Hydrogenase and Ni(III) Model Compounds. The combined FT-IR and EPR data indicate that our "as-isolated" *D. gigas* hydrogenase sample is primarily in form A. From its characteristic EPR signal (*g* values: 2.32, 2.23, 2.01),[63] this species is most frequently assigned as a Ni(III) complex. However, there is inevitably some charge delocalization onto the ligands, and in the extreme this same species could be viewed as a Ni(II) ligand−radical complex. L-edge spectroscopy is one technique that can help characterize the electronic structure of transition-metal complexes and the degree of configuration interaction. To address these issues, we have examined spectra for a variety of ionic and covalent Ni(III) complexes.

Ionic Ni(III) complexes such as $K_3Ni^{III}F_6$, $Li[Ni^{III}(\kappa^4\text{-mac*})]$, and $[Ni^{III}(cyclam)]Cl_2(ClO_4)$ exhibit a distinct low energy peak below the main L_3 maximum (Figure 4). Similar features were observed recently for Ni(III), $NdLiNiO_4$, and a ligand field multiplet calculation with mixing of ionic Ni(III) and Ni(II)−ligand hole configurations was able to reproduce the spectrum.[64,65] We include a simpler calculation without configuration interaction in Figure 4. Hu and co-workers point out that it is unwise to assign a particular final state configuration to a particular peak.[64] Still, these spectra illustrate how different hydrogenase form A is from Ni(III) complexes with "hard" (σ-donor) ligands.

For more covalent Ni(III) complexes such as those with sulfur donor ligands, the multiplet structure is unresolved and the L_3 absorption centroid moves ~0.5 eV lower to ~854 eV.[33] These complexes clearly have a significant amount of Ni(II) ligand hole character, which will be discussed more quantitatively in another publication. Because these spectra lack distinct multiplet features, it is difficult to draw any conclusions from spectral simulations. For the moment, we simply note that the "as-isolated" hydrogenase L-edge strongly resembles spectra for Ni(III) model compounds with sulfur donors, such as $[Ni^{III}pdtc_2]^-$.

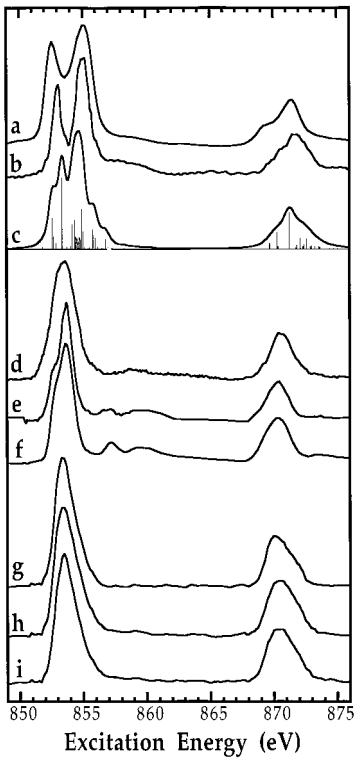

Figure 4. Comparison of oxidized *D. gigas* spectra with those of Ni(III) model compounds. Top to bottom: ("ionic Ni(III)") (a) $K_3Ni(III)F_6$, (b) $Ni^{III}(cyclam)Cl_2(ClO_4)$, and (c) simulation of a Ni(III) L-edge spectrum using D_{4h} symmetry, with $10Dq = 2.5$ eV and $D_s = 0.4$ eV. Covalent complexes: (d) $[Ni^{III}pdtc_2]^{2-}$, (e) $(n\text{-}Bu_4)Ni^{III}[S_2C_2(CF_3)_2]_2$, and (f) $(Et_4N)[Ni^{III}(S_2C_2Ph_2)]_2$. The as-isolated *D. gigas* hydrogenase spectra using bare (g), capped (h), and sealed (i) methods.

As documented in Figure 4, we found that the as-isolated spectrum did not depend on how the sample was introduced into the soft X-ray chamber.

Ni(II) Model Compounds. L-edge spectra for a variety of Ni(II) complexes are shown in Figure 5. Theoretical calculations have shown that high-spin and low-spin Ni compounds can be distinguished by several features of their Ni L-spectra. The "branching ratio", the ratio of integrated L_3 intensity to overall L-edge intensity, is significantly higher for high-spin compounds.[66] For the high-spin model compounds shown in Figure 5, this ratio varies from 0.76 for trigonal bipyramidal $Ni^{II}(terpy)(S\text{-}2,4,6\text{-}(i\text{-}Pr)_3C_6H_2)_2$, $Ni^{II}(terpy)(2,4,6\text{-}(Me)_3C_6H_2Se)_2$, and octahedral doped Ni/MgO to 0.72 for $Ni^{II}(cyclam)Cl_2$. The L_3-edge absorption maxima for high-spin Ni(II) compounds are generally lower in energy than for low-spin Ni(II) compound spectra, although the centroids often have about the same energy.[29] Finally, high-spin Ni(II) L-edge spectra often contain resolved multiplet structure, such as a high energy shoulder or resolved peak at the L_3-edge and broadening or splitting of the L_2-edge.

Ni(II) complexes with relatively ionic environments show the most pronounced multiplet structure.[30] To illustrate this point, we include in Figure 5 data for NiO, NiF_2, $[Ni(tren)_2](BF_4)_2$, and Ni-doped MgO. In these spectra, there is a resolved secondary peak on the high energy side of the L_3-edge and two distinct maxima at the L_2-edge. Octahedral Ni(II) L-edges have been extensively analyzed and simulated in the literature.[28,30,62,67,68] According to deGroot, the splitting of the L_3-edge in these cases is most profoundly affected by values of the Slater integrals F^2_{pd}, G^1_{pd}, and G^3_{pd}.[58] In qualitative terms, the L_3-edge main

(62) van der Laan, G.; Thole, B. T.; Sawatzky, G. A.; Verdaguer, M. *Phys. Rev. B* **1988**, *37*, 6587−6589.

(63) Cammack, R.; Fernandez, V. M.; Hatchikian, E. C. In *Inorganic Microbial Sulfur Metabolism*; LeGall, J., Peck, H. D., Jr., Eds.; pp 43−67, Academic Press Inc.: San Diego, CA, 1994; Vol. 243.

(64) Hu, Z.; Kaindl, G.; Warda, S. A.; Reinen, D.; deGroot, F. M. F.; Müller, B. G. *Chem. Phys.* **1998**, *232*, 63−74.

(65) Although in the Hu et al. paper Nd_4LiNiO_8 is referred to as low-spin, it turns out to be a high-spin, tetragonally distorted Ni(III) species. (F. deGroot, personal communication.)

(66) Thole, B. T.; van der Laan, G. *Phys. Rev. B* **1988**, *38*, 3158−3171.

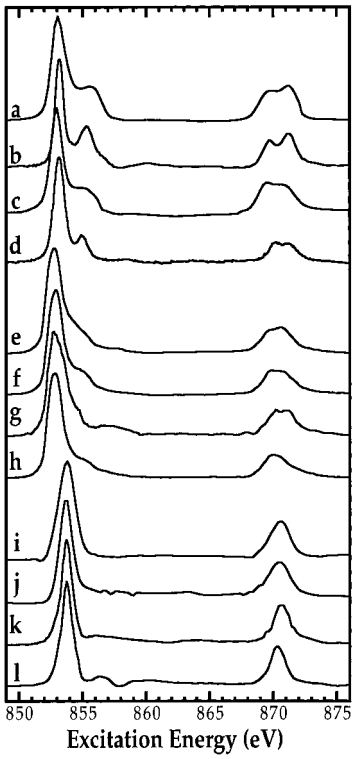

Figure 5. Representative spectra of high-spin and low-spin Ni(II) model compounds. (Top to bottom): (ionic high-spin complexes) (a) NiF_2, (b) Ni-doped MgO, (c) NiO, $[Ni(tren)_2](BF_4)_2$, and (d) $[Ni(tren)_2](BF_4)_2$; (more covalent high-spin complexes) (e) $Ni^{II}(DAPA)Cl_2$, (f) $Ni^{II}(DAPA)(SePh)_2$, (g) $Ni^{II}L_{S2}(Me)N_3(Pr)$, and (h) $Ni^{II}(terpy)(2,4,6\text{-}(Me)_3C_6H_2Se)_2$; (low-spin complexes) (i) Ni^{II}"S_4", (j) $[Ni^{II}_2$"LS1"$](ClO_4)_2$, (k) $[Ph_4P]_2Ni^{II}(MAC^*)$, and (l) $Ni^{II}diene(ClO_4)_2$.

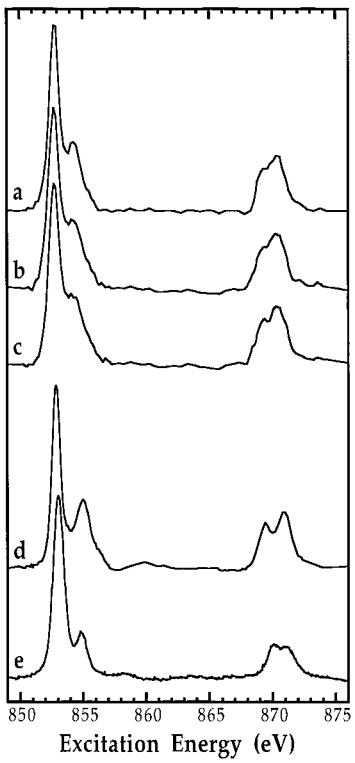

Figure 6. Comparison of H_2-reduced *D. gigas* hydrogenase spectra with model compound spectra. Top to bottom: (a) H_2-reduced *D. gigas* (*Dg*) H_2ase prepared bare on sapphire plate, (b) H_2-reduced *Dg* H_2ase on sapphire plate using capped method, (c) H_2-reduced *Dg* H_2ase prepared using sealed method, (d) doped Ni/MgO recorded with fluorescence detection, and (e) $[Ni(tren)_2](BF_4)_2$ recorded by electron yield.

peak and secondary peak arise from final states with a valence shell hole spin parallel or antiparallel to the core−shell hole spin. For high-spin Ni(II) with S, Cl, or Se ligands, the splittings between multiplet features diminish (Figure 5). The peak on the high energy side of the L_3-edge becomes an unresolved shoulder, and the maxima at the L_2-edge are no longer resolved.

For completeness, we include in Figure 5 a number of low-spin Ni(II) spectra. The relative intensity of the L_2 region increases compared to the L_3 region, resulting in lower branching ratios. For the low-spin model compounds that we have studied, this ratio varies from 0.63 for the tetragonal $[Ni^{II}(cyclam)](ClO_4)_2$ to 0.70 for $Ni^{II}L_{S5}$.[33] The spectra in general become sharper, especially in the L_2 region. The L_3 maximum generally appears at higher energy than for high-spin complexes, presumably because the single vacant *d*-orbital has been raised to a higher energy by the ligand field.

H_2-Reduced Hydrogenases—Comparison with Models and Simulations. The L-edge spectra for *D. gigas* hydrogenase samples are compared with model compounds and simulations in Figure 6. H_2-reduced *D. gigas* hydrogenase has a spectrum with a distinct secondary peak on the high energy side of the L_3-edge, as well as a partially resolved splitting in the L_2-edge. The L_3 centroid is at 853.6 and the branching ratio is 0.76. Similar spectra were obtained whether the samples were prepared bare on sapphire or by using the capped or sealed methods (Figure 6). At first glance, thanks to the resolved secondary peak at the L_3-edge, the H_2-reduced spectra appear closer to the ionic model compounds. However, with four sulfur ligands at the Ni site, one would expect greater correspondence with the more covalent Ni(II) models.

On closer inspection, we find that the peak-to-peak splitting varies from 2.5 eV in NiF_2, to 2.1 eV in Ni-doped MgO, to 1.75 eV in $[Ni^{II}(tren)_2]^{2-}$. In general, the less ionic the environment, the smaller the multiplet splitting.[30] The splitting in the H_2-reduced spectra is 1.6 eV. This smaller splitting is thus consistent with the more covalent Ni environment, and the only discrepancy seems to be the relative peak intensities. DeGroot and co-workers have pointed out that fluorescence-detected excitation spectra (used for the protein data) and total electron yield data (used for the model compounds) are not expected to be exactly the same.[69,70] This may explain some of the differences in peak intensities between hydrogenase and the model compounds. Still, from the L_3-edge peak and centroid positions,[30] along with the L_3 shoulder and the split L_2-edge, there is little doubt that the sample being probed in the X-ray experiment is high-spin Ni(II).

Dithionite-Reduced and CO-Inhibited Hydrogenase. In Figure 7 we show L-edge spectra for dithionite-reduced and CO-inhibited *D. gigas* hydrogenase. The latter sample was recorded by the sealed method under a CO atmosphere to avoid dissociation of the CO during sample transfer. The L_3 centroids are 853.6 and 853.5 eV and the branching ratios are 0.76 and 0.75 for dithionite-reduced and CO-inhibited samples, respectively. All of the characteristic features of high-spin Ni(II) are

(67) van Elp, J.; Searle, B. G.; Sawatzky, G. A.; Sacchi, M. *Solid State Commun.* **1991**, *80*, 67−71.
(68) van Elp, J.; Eskes, H.; Kuiper, P.; Sawatzky, G. A. *Phys. Rev. B* **1992**, *45*, 1612−1622.
(69) deGroot, F. M. F.; Arrio, M.-A.; Sainctavit, P.; Cartier, C.; Chen, C. T. *Solid State Commun.* **1994**, *92*, 991−995.
(70) deGroot, F. M. F.; Arrio, M.-A.; Sainctavit, P., C., C.; Chen, C. T. *Physica B* **1995**, *208−209*, 84−86.

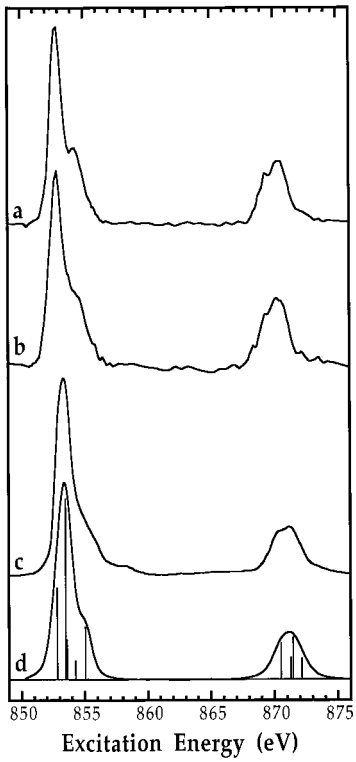

Figure 7. Additional L-edge spectra. Top to bottom: (a) dithionite-reduced *D. gigas* hydrogenase using capped method and (b) CO-inhibited *D. gigas* hydrogenase using sealed method, (c) Ni^{II}(DAPA)-$(SePh)_2$, and (d) ligand field multiplet simulation for Ni(II) using D_{3h} symmetry and 10Dq = 1.5 eV.

again present, and we can exclude Ni(I) as a significant component in these samples.

The L_3-edge shoulder for the CO samples is the weakest of all the reduced samples, suggesting a different ligand field compared to forms R_{film} and SU. Reduced multiplet splittings in this spectrum indicate a more covalent environment, which is consistent with CO binding to Ni. Although it is certainly not a structural model, the spectrum of trigonal bipyramidal Ni^{II}(DAPA)$(SePh)_2$[45] resembles the CO-inhibited enzyme and illustrates the reduced splittings seen in a more covalent environment. The latter spectrum can be simulated by multiplet calculations in (D_{3h}) symmetry (Figure 7).

Discussion

The main findings of this work are that (1) form A samples of Ni−Fe hydrogenase exhibit a spectrum consistent with covalent Ni(III), (2) both fully reduced forms, unready (SU) and reduced (R), contain high-spin Ni(II), and (3) the CO-inhibited enzyme also contains high-spin Ni(II). These conclusions are based on the L-edge peak and centroid positions, the branching ratios, and the L-edge multiplet structure. The conclusion with regard to form A is hardly controversial, since Ni(III) has been proposed as the best description of form A virtually since the discovery of its distinct EPR signal.[71] From comparison with ionic and covalent model compound spectra, the L-edge data show that the enzyme is near the extreme end of covalent Ni(III) complexes.

Our evidence for high-spin Ni(II) in the reduced forms of hydrogenase is at odds with the conclusions from previous studies, which have frequently assigned these states as low-spin Ni(II).[16,60,72−75] However, the argument for low-spin Ni(II) consists primarily of negative results. No UV−visible MCD effect was found for forms SI and R in *C. vinosum* hydrogenase[76] or from reduced forms of *D. gigas* and *M. thermoautotrophicum*.[73] Attempts to find a parallel mode EPR signal in Ni-R *D. gigas* hydrogenase were unsuccessful.[72] A saturation magnetization study of the native *D. baculatus* enzyme also concluded that the Ni is diamagnetic.[74] Finally, the average Ni-S bond length found by EXAFS for form R *D. gigas* hydrogenase was ∼2.2 Å.[27] It has been argued that this is much closer to the 2.16−2.21-Å range found for low-spin 4-coordinate thiolate complexes than to the 2.39−2.53-Å range found for 6-coordinate thiolate complexes.[16]

The spin state of a Ni(II) complex will of course depend on the strength and symmetry of the ligand field, which can in turn be inferred from the molecular structure.[77] Although a crystal structure is not yet available for form R of the *D. gigas* enzyme, the reduced *D. baculatum* hydrogenase structure is expected to be similar, apart from the substitution of selenocysteine for one cysteine at the active site.[8] The structure of the reduced *D. vulgaris* Miyazaki enzyme should also be relevant.[10] In both of the reduced crystal structures, there are only four observable ligands to Ni. (There may also be one or two H ligands.) The average Ni-S bond length in the *D. vulgaris* structure is 2.33 Å,[10] while for *D. baculatum* the Ni-S/Se average is 2.415 Å.[8] In the latter structure, the individual Ni-S bond lengths of 2.25, 2.33, and 2.62 Å are too different to be modeled by a single average Ni-S distance in an EXAFS simulation. When a metal coordination sphere is highly distorted, EXAFS analysis will heavily weight the shortest bond lengths, and the calculated distance will not be a true arithmetic average. This could explain why the ∼2.2-Å EXAFS Ni-S bond lengths are shorter than the crystallographic values.

Both groups involved with the crystal structures assume that the coordination position that was filled in the oxidized structure is not really vacant in the reduced structure but is instead filled by a bridging hydride.[8,10] This leads to at least 5-coordinate Ni, in geometries that could be square pyramidal or trigonal bipyramidal. Density functional calculations by Amara and co-workers suggest the presence of an additional terminal hydride on Ni (as well as the bridging hydride)—thus an approximately octahedral site.[78] The XANES region has also been interpreted as evidence for 6-coordinate Ni.[27] Another density functional study found a square planar Ni-R site with a hydrogen molecule on the Fe center.[75] There is clearly no consensus on the Ni-R geometry.

Ni(II) complexes easily undergo structural and conformational changes as a function of temperature, anion, and solvent condition.[79] Coyle and Stiefel have pointed out that some 5-coordinate Ni(II) complexes can adopt both square pyramidal and trigonal bipyramidal geometries.[77] The difference in the two geometries only requires small motions of the ligands, but often

(71) Albracht, S. P. J.; Kalkman, M. I.; Slater, E. C. *Biochim. Biophys. Acta* **1983**, *724*, 309−316.

(72) Dole, F.; Fournel, A.; Magro, V.; Hatchikian, E. C.; Bertrand, P.; Guigliarelli, B. *Biochemistry* **1997**, *36*, 7847−7854.

(73) Kowal, A. T.; Zambrano, I. C.; Moura, I.; Moura, J. J. G.; LeGall, J.; Johnson, M. K. *Inorg. Chem.* **1988**, *27*, 1162−1166.

(74) Wang, C. P.; Franco, R.; Moura, J. J. G.; Moura, I.; Day, E. P. *J. Biol. Chem.* **1992**, *267*, 7378−7380.

(75) Niu, S.; Thomson, L. M.; Hall, M. B. *J. Am. Chem. Soc.* **1999**, *121*, 4000−4007.

(76) Cheesman, M. Ph.D. Thesis, University of East Anglia, 1989.

(77) Coyle, C. L.; Stiefel, E. I. In *The Bioinorganic Chemistry of Nickel*; Lancaster, J. R., Jr., Ed.; VCH Publishers: New York, 1988; pp 1−28.

(78) Amara, P.; Volbeda, A.; Fontecilla-Camps, J. C.; Field, M. J. *J. Am. Chem. Soc.* **1999**, *121*, 4468−4477.

(79) Cotton, F. A.; Wilkinson, G.; Murillo, C. A.; Bochmann, M. *Adv. Inorg. Chem.*, Wiley-Interscience: New York, 1999.

results in different Ni spin states. It seems possible that slight perturbations of the hydrogenase active site could also modulate the Ni spin state, and this sensitivity might be relevant to the catalytic mechanism. It is obvious that additional work is needed to better define the structure of Ni-R and the other active intermediates.

Summary

Nickel L-edge X-ray absorption spectroscopy has been combined with FT-IR spectroscopy to study three different Ni−Fe hydrogenases under a variety of conditions. FT-IR of partially dried *D. gigas* films yielded spectra very similar to previously reported data for homogeneous solutions of forms A, SU, and R and CO-inhibited enzyme. FT-IR of *D. baculatus* and *P. furiosus* samples showed that they contain a number of species, and additional work is needed to produce homogeneous films of these enzymes. The *D.gigas* enzyme form A has an L-edge spectrum consistent with a covalent Ni(III) species. All of the spectral features for the H_2-reduced form R_{film}, the dithionite-reduced form SU, and the CO-inhibited *D. gigas* enzyme indicate high-spin Ni(II). Control of the Ni spin state may be one means by which nature modulates the catalytic active of Ni sites in enzymes.

Acknowledgment. We thank Dr. Frank deGroot for many valuable discussions and Prof. Rosemary Smith at UC Davis for providing the silicon nitride membranes. This work was supported by the Department of Energy, Office of Biological and Environmental Research, and the National Institutes of Health grant GM-44380 (for S.P.C.). The Stanford Synchrotron Radiation Laboratory, the National Synchrotron Light Source, and the Advanced Light Source are supported by the Department of Energy, Office of Basic Energy Sciences.

JA000945G